

# Classical condensation of light pulses in a loss trap in a laser cavity

GILAD OREN, ALEXANDER BEKKER, AND BARUCH FISCHER\*

Department of Electrical Engineering, Technion, Haifa 32000, Israel

\*Corresponding author: fischer@ee.technion.ac.il

Received 23 April 2014; revised 15 July 2014; accepted 29 July 2014 (Doc. ID 210707); published 2 September 2014

**We present an experimental demonstration of condensation in a many-light-pulse system in a loss trap (loss well) in a one-dimensional laser cavity. The route to condensation is similar to Bose–Einstein condensation in a potential trap (potential well), but classical. The pulses, their loss levels, and the noise-induced power distribution take the role of “particles”, “energy” levels, and quantum-thermal population-statistics, respectively. The multipulse system is formed by high harmonic active mode-locking modulation and the trap by an envelope modulation. The experiment is done with an erbium-doped fiber laser. Condensation is shown to occur when the loss trap has near the lowest-loss pulse a power law dependence with exponent smaller than 1, as the theory predicts.** © 2014 Optical Society of America

**OCIS codes:** (140.4050) Mode-locked lasers; (270.3430) Laser theory; (020.1475) Bose-Einstein condensates; (000.6590) Statistical mechanics.

<http://dx.doi.org/10.1364/OPTICA.1.000145>

Bose–Einstein condensation (BEC) is a special many-boson phenomenon that was observed in atomic particles [1,2]. Recent works have shown condensation in relatively simple systems, even at room temperature, compared to the ultralow temperatures needed so far to observe BEC. They were mostly based on nonatomic particles such as photons [3], polaritons [4,5], and magnons [6]. We can also find classical condensation experiments that use light and lasers [7–13]. This was shown, for example, in a single-pulse waveform system in an actively mode-locked laser, where the light power collapses upon condensation into the lowest pulse waveform [7,8]. In a more recent work [9], we theoretically suggested that simple cw lasers show in certain conditions a classical light

condensation (LC) route that is formally similar to quantum BEC [14]. This is based on weighting the modes of the laser in a loss–gain scale, compared to energy (or photon frequency) in BEC, and the noise in the laser (spontaneous emission, external, etc.) functions as temperature. The levels are the regular cavity modes of the laser, and the condensation occurs in the modes’ spectral domain where, for low noise or high laser power, the light power concentrates at the lowest-loss mode. The relation of this effect to lasing and to photon-BEC [3] was discussed in [9]. Other many-body effects such as phase transitions and critical phenomena were also observed in lasers [15–19].

Our experiment is done with a unique many-body system of many pulses in a laser cavity. The “particles”, their “energy” levels, and population are the pulses, their corresponding loss levels, and powers, respectively. As we discuss below, this pulse system is formally equivalent to the cw laser mode system with spectral filtering that was theoretically shown to exhibit LC [9]. In the present pulse system, however, the condensation is expected to be in the spatial (or time) domain rather than the frequency domain. This condensation prediction has not been observed yet experimentally, and the present work therefore provides a first experimental demonstration of it. It requires a loss trap (loss well) with a power law dependence having an exponent  $\eta < 1$ , like the potential trap (potential well) needed for atomic quantum BEC in one dimension (1D) [14]. There (and in single-pulse condensation)  $\eta < 2$  due to an additional kinetic energy (or similar) term.

The many-pulse system is obtained by the  $N_0$ -th harmonic active mode locking (AML) order of a laser that generates  $N_0$  pulses with approximately the same width and power, bouncing in the cavity with equal spacing. AML is usually obtained by RF-driven electro-optic modulation of the light in the laser at the basic or harmonic cavity frequency that can nowadays reach 40 GHz, and then generate pulse trains at such rates. In fiber lasers with lengths of  $L \sim 10$ – $100$  m, we can have with high harmonic modulations hundreds and thousands of pulses in the cavity. We can view the pulses in the time domain or in the corresponding spatial domain in the cavity when we take a snapshot of the pulses or propagate with them. We therefore

have in the cavity  $N_0$  pulse sites given by the harmonic AML with a pulse population in terms of power. We nevertheless need hierarchy in the pulse system, like the energy in thermodynamics statistics. We therefore add to the usual AML  $N_0$  pulse system in the cavity an envelope modulation that makes the pulses have different losses, as illustrated in Fig. 1 for  $N_0 = 15$  pulses. This modulation can be viewed as a loss trap, like the potential trap in BEC [14]. It determines the density of pulse loss states that has an important role for condensation occurrence. The situation in the pulse system is similar to that of the cw laser mode case, where a loss trap in the spectral domain (spectral filtering) can produce LC [9]. Another important point here is that each pulse state is represented by a single loss value according to its location in the loss trap (as seen in Fig. 1). By doing this, we ignore the high intrapulse

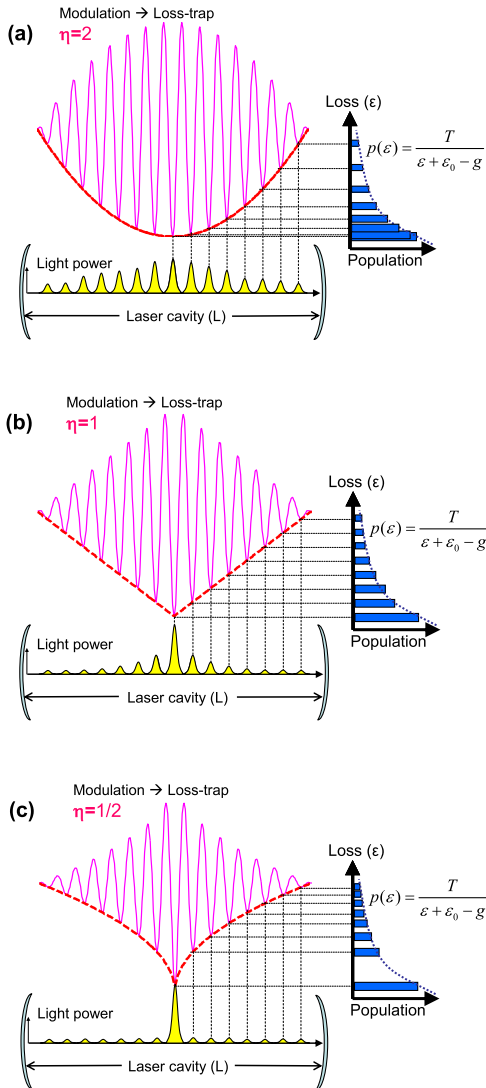


**Fig. 1.** Pulse system and the loss trap in the laser cavity. The loss trap is provided by an envelope modulation, shown for  $\eta = 2, 1, 1/2$ , and the pulses by a harmonic modulation, here illustrated for a 15th order, that gives 15 pulse sites. Characteristic pulse forms are plotted in the cavity in each figure along with their power distributions, which are shown in the diagrams to the right. We note that in the experiments, the pulses in the cavity are much denser, and so are the loss states. In the present experiment, we had 51 pulses.

loss levels and take only the lowest one in each pulse; it is allowed for pulse forms (commonly harmonic oscillator modes) with loss level spacings that are significantly larger than the interpulse loss level difference. A detailed study of this point will be given elsewhere.

We summarize the mathematical base of pulse condensation in the regime that each pulse has one loss value. We recall that the pulses are produced by high harmonic AML with an added envelope modulation that produces the loss trap and the pulse loss differentiation. We take the pulse locations in the cavity as a grid where the pulses are located with a population size measured in power terms, according to the noise-induced statistics. Therefore, the equation of motion is considered for the pulse population in the cavity without going into the formation of the pulses by high harmonic mode locking. Then the master equation for the pulse amplitudes  $a_m$  and the mathematical description are similar to the theory developed for the cw laser mode system [9]:

$$(da_m/d\tau) = (g - \varepsilon_m)a_m + \Gamma_m. \quad (1)$$

Here,  $a_m$  denotes pulse amplitude compared to mode amplitudes in the cw laser case,  $\tau$  is the long-term time variable that counts cavity roundtrip frames, and  $g$  is a slow saturable-gain factor, shared by all pulses.  $\varepsilon_m$  is the  $m$ th pulse loss term, and  $\Gamma_m$  is an additive noise term that can result from spontaneous emission and any other internal or external source. It is modeled by a white Gaussian process with covariance  $2T$ :  $\langle \Gamma_m(\tau)\Gamma_n^*(\tau') \rangle = 2T\delta(\tau - \tau')\delta_{mn}$  and  $\langle \Gamma_m(\tau) \rangle = 0$ , where  $\langle \rangle$  denotes average. We emphasize that the master equation has a noise term but no explicit nonlinearity besides the one resulting from the overall power constraint.

We obtain from Eq. (1) the following expression for the overall pulse power in the cavity:

$$P = \sum_{m=-N}^N p_m = \sum_{m=-N}^N \frac{T}{\varepsilon_m - g} \\ \rightarrow P = \frac{T}{\varepsilon_0 - g} + T \int_0^{\varepsilon_N} \frac{\rho(\varepsilon)d\varepsilon}{\varepsilon + \varepsilon_0 - g}, \quad (2)$$

where  $p_m = |a_m|^2$  is the power of pulse  $m$ . For the integral with the continuous loss variable  $\varepsilon$ , measured relatively to the lowest pulse loss  $\varepsilon_0$ , we define the density of loss states (DOS)  $\rho(\varepsilon)$  that has a prime role for condensation occurrence.  $\varepsilon_N$  is the highest pulse loss in the cavity, the loss trap depth. The first term at the right-hand side in the second line of Eq. (2) gives the power of the lowest-loss mode, and the second term is the power in all higher modes. We can notice the resemblance of Eq. (2) to that of the overall boson number in a potential well in BEC [14]. The weight for each spectral component depends on  $\rho(\varepsilon)$  and the factor  $T/(\varepsilon + \varepsilon_0 - g)$  replaces the Bose–Einstein statistics (see Table 1). The power of each pulse is  $p_m = T/(\varepsilon_m - g)$ , meaning that the noise populates the pulse states according to their loss in a similar way to thermal excitation via Bose–Einstein distribution.

We consider for the envelope loss function a power law dependence around the lowest-loss pulse,  $\varepsilon_m = \varepsilon_0 + \varepsilon_N|(m/N)|^\eta$ ,

**Table 1. Analogy between BEC and Pulse/Mode Condensation**

Quantum BEC in a Potential Trap [14]		Classical Pulse/Mode Condensation in a Loss Trap
Many noninteracting bosons		Many noninteracting pulses/modes in a laser cavity
Energy scale:	$\epsilon, h\nu$	Loss scale: $\epsilon$
Temperature:	$T$	Optical noise: $T$
Bose–Einstein thermal statistics:		Noise-induced pulse/mode power distribution:
	$f_{\text{BE}}(\epsilon) = 1/\{\exp[(\epsilon - \mu)/k_B T] - 1\} \xrightarrow{[(\epsilon - \mu)/k_B T] \ll 1} k_B T/(\epsilon - \mu)$	$p(\epsilon) = T/(\epsilon + \epsilon_0 - g)$
Chemical potential:	$\mu$	Lowest pulse loss (“chemical-potential”): $\mu \equiv g - \epsilon_0$
Overall particle number constraint:		Overall power constraint:
	$N = n_0 + \int_0^\infty \frac{\rho(\epsilon)d\epsilon}{\exp[(\epsilon - \mu)/k_B T] - 1}$	$P = p_0 + T \int_0^{\epsilon_N} \frac{\rho(\epsilon)d\epsilon}{\epsilon + \epsilon_0 - g}$
$n_0$ is the ground-state ( $\epsilon = 0$ ) population.		$p_0$ is the lowest-loss ( $\epsilon = 0$ ) pulse/mode power.
Energy DOS in 1D potential trap [14]: $\rho(\epsilon) \propto \epsilon^{(1/\eta) - (1/2)}$		Pulse/mode DOS in 1D loss trap [9]: $\rho(\epsilon) \propto \epsilon^{(1/\eta) - 1}$
DOS for d-dimensional potential trap [14]: $\rho(\epsilon) \propto \epsilon^{(d/\eta) + (d/2) - 1}$		Single-pulse AML DOS in 1D loss trap [7,8]: $\rho(\epsilon) \propto \epsilon^{(1/\eta) - (1/2)}$
Condition for condensation in 1D potential trap [14]: $\eta < 2$		Condition for pulse/mode condensation in 1D loss trap [9]: $\eta < 1$
		Condensation condition for single-pulse AML in 1D [7,8]: $\eta < 2$

where we have  $N_0 = 2N + 1$  pulses in the cavity. It can be expressed in a continuous variable form  $\epsilon = \epsilon_N (|t|/t_R)^\eta = \epsilon_N (|z|/L)^\eta$  in terms of the cavity time  $t/t_R$  or space  $z/L$  variables.  $L = ct_R$  and  $t_R$  are the roundtrip cavity length and time, and  $c$  is the speed of light. Loss traps with various exponents  $\eta$  are shown in Fig. 1. The corresponding DOS, derived as in [9], is given by  $\rho(\epsilon) = [2N/(\eta\epsilon_N^{1/\eta})]e^{(1/\eta) - 1}$ .

As the noise  $T$  is lowered (or  $P$  is raised) the distribution  $p(\epsilon)$  yields a gradual concentration of the pulse power at lower-loss states. Nevertheless, when condensation takes place,  $p_0$  gets a macroscopic part of the power. It occurs when the integral in Eq. (2) converges at  $\epsilon = 0$  ( $t = z = 0$ ), which happens when  $\eta < 1$ . Then, the power population of the light at higher than  $\epsilon = 0$  levels stays unchanged (filled) at  $P_c = T \int_0^{\epsilon_N} \rho(\epsilon)d\epsilon/\epsilon$ , and additional pumping that increases  $P$  beyond  $P_c$  (or lowering  $T$  below  $T_c$ ) will cause population of the lowest-level power  $p_0$ , which starts to grow macroscopically. At condensation ( $P \geq P_c$  or  $T \leq T_c$ ), the net gain for the lowest-loss pulse (the “chemical potential”) becomes  $\mu \equiv g - \epsilon_0 = 0$ . (It is negative at the noncondensate regime.) We therefore have a many-pulse system with a condensation route that is mathematically similar to BEC, but classical. As in BEC, there is no direct pulse (“particle”) interaction, but a global constraint on the overall pulse power (“particle number”). Nevertheless, the “energy” hierarchy is in a loss–gain scale, where the “ground state” is the lowest-loss pulse and the noise has the role of temperature.

Our experiment is done in a ring erbium-doped fiber laser described in Fig. 2, with a 51st order harmonic AML that gives 51 pulses equally spaced in the cavity and has about the same power before applying the envelope modulation. We injected into the cavity controllable optical noise  $T$  using amplified spontaneous emission from an erbium-doped fiber amplifier.

Figure 3 gives the experimental and theoretical condensation ratio  $p_0/P$  dependence on the noise level  $T$  for several exponents. The condensation transition becomes sharper when the pulse number increases, as is the case in many-body

systems.  $T$  measures the injected noise, but in the experiment there is the additional internal laser noise that limits the lowest achievable overall  $T$  and therefore the maximum condensation ratio. In the theoretical analysis, we added a constant internal noise that fitted the experimental graphs (which is negligible at the condensation region, but becomes significant at low  $T$ ) that caused a partial condensation ratio and its saturation, as seen in this figure and in Fig. 4. We also note that the plots are against  $T/P$  (with an arbitrary shift) since variation of the injected noise in the experiment changed  $P$ , although the laser pumping was kept unchanged.

Figure 4 shows measurements of the power distributions among the 51 pulses in the cavity, as a function of the injected noise level  $T$ , for various exponents. In all of them, the distribution becomes more centered at lower-loss pulse states when the noise is lowered, as expected in noise-induced (or thermal) excitation. However, for  $\eta < 1$  and partially for  $\eta = 1$ , there is a pronounced transition of the power into

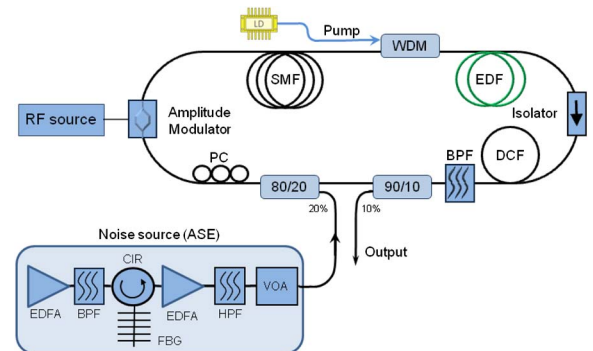


**Fig. 2.** Experimental setup. Ring fiber laser of length  $L \approx 404$  m, with a high harmonic AML, an envelope modulation (509 kHz), and a controllable noise injection. The wavelength was  $\sim 1549$  nm. The system is composed of an erbium-doped fiber amplifier (EDFA), single mode fiber (SMF), wavelength division multiplexer (WDM), dispersion compensation fiber (DCF), bandpass filter (BPF), high pass filter (HPF), variable optical attenuator (VOA), polarization controller (PC), circulator (CIR), and fiber Bragg grating (FBG).

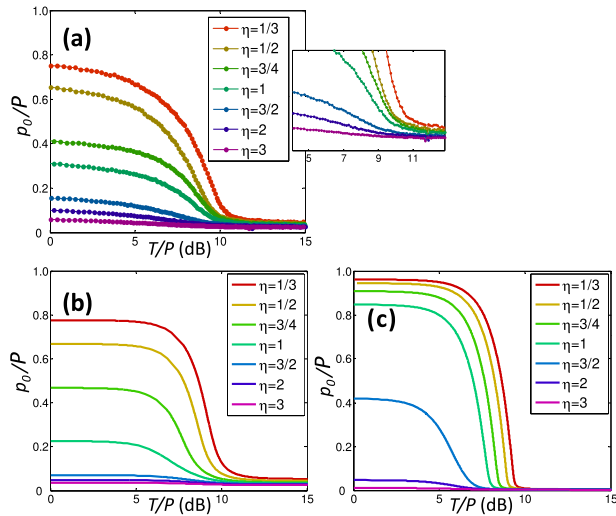


**Fig. 3.** Experimental and theoretical lowest-loss pulse power versus noise level normalized by power ( $T/P$ ) for various  $\eta$  s. (a) Experimental results for 51 pulses in the cavity. The inset is a zoomed view of the transition region and the difference between the two regimes, below and above  $\eta = 1$ . Theoretical graphs are shown for (b) 51 and (c) 501 pulses.

the lowest-loss pulse state. The experimental results in Figs. 3 and 4 follow and verify the theoretical prediction [9] showing condensation for  $\eta < 1$ . We note in the caption of Fig. 3 that  $T$  measures the injected and not the internal noise,

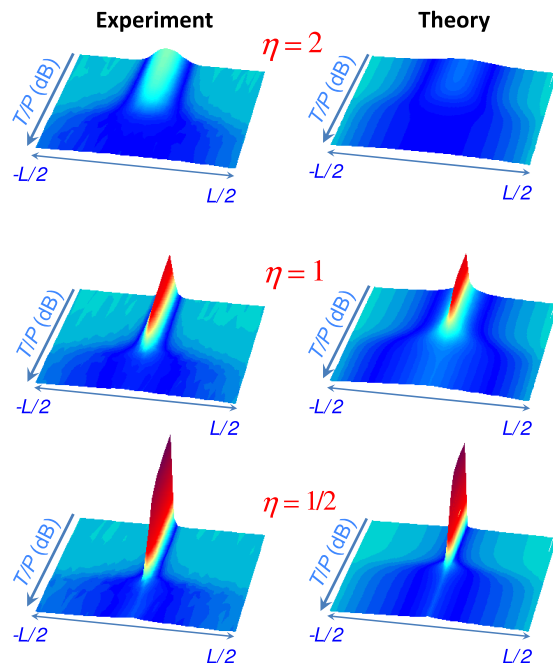


**Fig. 4.** Experimental and theoretical pulse power distribution. The experimental figures (left-hand side figures) are plotted from measurements of 51 equally spaced pulses in the cavity frame  $(-L/2, L/2)$ , as a function of the injected noise level  $T$  (in logarithmic scale and opposite direction), for various  $\eta$  s. The corresponding theoretical results are shown in the right-hand side figures. We can see the route to condensation for  $\eta < 1$  with a massive lowest-loss pulse population as  $T$  decreases. The power scale is the same as in Fig. 3.

and therefore the figures show partial condensation ratios and saturation. A detailed account on those sides will be included in a full-length work. We also note that in our experiment we had only 51 pulses in the cavity, and therefore the phase-transition point is less sharp and the higher-loss pulse powers are not close to zero as one would obtain in the thermodynamic limit for large particle number, as can be seen in Fig. 3(c), which was calculated for 501 pulses. A larger number of pulses in the cavity would be experimentally feasible, but it raised other disturbances in the present experiment.

We have experimentally demonstrated and verified the prediction of a classical condensation phenomenon with a pulse system in a 1D laser cavity in a loss trap. The route to condensation is similar to cw laser LC and formally similar to quantum BEC in a potential trap [14]. We have experimentally shown that condensation occurs for loss trap exponents  $\eta < 1$  like in the BEC case. The experiment is done with a fiber laser that produces pulses upon high harmonic AML, and the loss trap is achieved by an envelope modulation. It is a remarkably simple experimental system that nevertheless provides a first demonstration of LC in a new many-pulse system in a loss trap in a laser cavity. It can also serve as an experimental base for a further study on condensation that includes, for example, nonlinearity and pulse interaction.

## FUNDING INFORMATION

Israel Science Foundation (ISF); Binational US-Israel Science Foundation (BSF).

## REFERENCES

1. M. H. Anderson, J. R. Ensher, M. R. Matthews, C. E. Weiman, and E. A. Cornell, *Science* **269**, 198 (1995).
2. A. J. Leggett, *Rev. Mod. Phys.* **73**, 307 (2001).
3. J. Klaers, J. Schmitt, F. Vewinger, and M. Weitz, *Nature* **468**, 545 (2010).
4. R. Balili, V. Hartwell, D. Snoko, L. Pfeiffer, and K. West, *Science* **316**, 1007 (2007).
5. H. Deng, G. Weihs, C. Santori, J. Bloch, and Y. Yamamoto, *Science* **298**, 199 (2002).
6. S. O. Demokritov, V. E. Demidov, O. Dzyapko, G. A. Melkov, A. A. Segre, B. Hillerbrands, and A. N. Slavin, *Nature* **443**, 430 (2006).
7. R. Weill, B. Fischer, and O. Gat, *Phys. Rev. Lett.* **104**, 173901 (2010).
8. R. Weill, B. Levit, A. Bekker, O. Gat, and B. Fischer, *Opt. Express* **18**, 16520 (2010).
9. B. Fischer and R. Weill, *Opt. Express* **20**, 26704 (2012).
10. C. Sun, S. Jia, C. Barsi, S. Rica, A. Picozzi, and J. W. Fleischer, *Nat. Phys.* **8**, 470 (2012).
11. C. Connaughton, C. Josserand, A. Picozzi, Y. Pomeau, and S. Rica, *Phys. Rev. Lett.* **95**, 263901 (2005).
12. C. Conti, M. Leonetti, A. Fratolocchi, L. Angelani, and G. Ruocco, *Phys. Rev. Lett.* **101**, 143901 (2008).
13. A. Fratolocchi, *Nat. Photonics* **4**, 502 (2010).
14. V. Bagnato and D. Kleppner, *Phys. Rev. A* **44**, 7439 (1991).
15. A. Gordon and B. Fischer, *Phys. Rev. Lett.* **89**, 103901 (2002).
16. B. Vodonos, R. Weill, A. Gordon, A. Bekker, V. Smulakovsky, O. Gat, and B. Fischer, *Phys. Rev. Lett.* **93**, 0153901 (2004).
17. A. Rosen, R. Weill, B. Levit, V. Smulakovsky, A. Bekker, and B. Fischer, *Phys. Rev. Lett.* **105**, 013905 (2010).
18. A. Schwartz and B. Fischer, *Opt. Express* **21**, 6196 (2013).
19. B. Fischer and A. Bekker, *Opt. Photon. News* **24**, 40 (2013).